

Growth of Al on GaAs(001): Observation of interfacial submonolayer structure

S. K. Donner, Rik Blumenthal, J. L. Herman, Rajender Trehan, Ehud Furman, and Nicholas Winograd

Pennsylvania State University, 152 Davey Laboratory, University Park, Pennsylvania 16802

(Received 9 January 1989; accepted for publication 17 August 1989)

Submonolayer structure has been observed using reflection high-energy electron diffraction during room-temperature deposition of Al onto (2×4) reconstructed GaAs(001) surfaces prepared by molecular beam epitaxy. This structure with a (4×1) symmetry occurs after ~ 0.25 monolayer of Al deposition. It is growth-rate independent, reproducible, and stable. This result shows that there is a strong, directionally dependent adatom-adatom interaction at submonolayer coverages.

The structure of metal-semiconductor interfaces in the low-coverage regime is an important factor in determining the electronic states responsible for Fermi level stabilization and in resolving the mechanism of Schottky barrier formation.¹ For Al on GaAs(110), Al adatom clusters, metallic and covalent chemisorption bonds,² as well as native or induced defects,^{3,4} have each been considered to influence the electronic structure of the interface (during the crucial stage when the Schottky barrier is forming). Photoemission and optical spectroscopies have shown that various electronic states exist at the interface including bulk-defect-related, As-related, and metal-specific states.⁵ On surfaces grown by molecular beam epitaxy (MBE) bulk-defect-related states have been shown to vary from a density sufficient to cause fully developed band bending prior to metal deposition⁶ to relatively defect-free MBE-grown GaAs(001) where band bending is minimal.⁷ Al-As covalent bonding at the Al/GaAs(001) interface has been confirmed by Auger electron spectroscopy (AES).⁸⁻¹⁰ The presence of metal-specific states has been suggested by a model which places Al atoms in interstitial positions at low coverage in the (110) direction and which physically matches the experimentally observed fcc Al(110) crystal to the GaAs(001) lattice. The dynamics of Al/MBE-GaAs(001) interface formation has also been extensively studied using AES, photoelectron spectroscopy, and reflection high-energy electron diffraction (RHEED). These techniques show that several layers of Al are required to attain films with bulk-like structures.⁶⁻¹⁵

In this letter, we provide the first experimental evidence that Al, during the initial stages of deposition, forms an ordered overlayer on GaAs(001). This stable and reproducible surface with (4×1) symmetry as examined by RHEED is found at coverages near 0.25 monolayer (ML) of Al on $(2 \times 4)/[c(2 \times 8)]$ [hereafter referred to as (2×4)] As-stabilized MBE-grown GaAs(001). These results are important since they show that both directionally dependent adatom-substrate interactions and strong adatom-adatom interactions are present in the low Al coverage regime and may be associated with the initial stages of Schottky barrier formation.

To ensure a high quality (001) surface, a $2 \mu\text{m}$ undoped epitaxial layer of GaAs was grown by MBE prior to *in situ* metallization. The Riber 2300 R&D MBE growth chamber is part of a thin-film deposition/surface analysis system de-

scribed previously.¹⁶ The pressure of the MBE is $< 3.0 \times 10^{-11}$ Torr after bakeout and before growth with liquid-nitrogen shrouds filled. Silicon-doped GaAs(001) wafers oriented to $\pm 0.5^\circ$ were obtained from MA/COM Laser Diode Inc. Substrates were degreased with trichloroethane, acetone, and methanol and etched with a 5:1:1 sulfuric acid:peroxide:water solution. The native oxide was removed during thermal treatment at 600°C under an As_4 flux. A (2×4) reconstruction could be formed by growing a semi-insulating buffer layer at a substrate temperature of $560\text{--}570^\circ\text{C}$, followed immediately by shuttering the As and Ga ovens. The (2×4) -(001)GaAs surface reconstruction has been shown to exist over a wide range of As coverages.¹⁷⁻¹⁹ The surfaces used in this work were prepared over a range of As-to-Ga beam equivalent pressure ratios from 9:1 to 15:1. Aluminum was deposited from an effusion oven onto the sample which was held at 25°C . The As background pressure was always reduced to less than 1×10^{-9} Torr prior to metal deposition. The Al deposition rates were determined from calibrated beam equivalent pressure ratios of Al to Ga. The calibration factors were determined from RHEED oscillations observed during GaAs(001) growth²⁰ and from the known difference in ion gauge sensitivity to Ga and Al.²¹ This deposition rate was 0.025 ML s^{-1} at an oven temperature of 1000°C . In this instance, we have arbitrarily defined 1 ML as being equal to the surface site density of Al(001) of $1.23 \times 10^{15} \text{ atoms cm}^{-2}$.

The analysis of MBE-grown GaAs reconstructions by RHEED is accomplished by examining the diffraction streaks resulting from an incident electron beam directed along at least two orthogonal azimuths.^{22,23} The RHEED patterns for clean (2×4) GaAs(001) in the $[110]$, $[100]$, and $[\bar{1}10]$ directions are shown in Fig. 1. An electron beam of 9.5 keV was incident on the sample at a glancing angle of less than 3° . The dynamic RHEED pattern was recorded on video tape and later analyzed. The sample was rotated every 2-3 s between perpendicular azimuths during the taping. Schematic representation of the RHEED patterns for the room-temperature (2×4) GaAs reconstruction before Al deposition and for various Al coverages is shown in Fig. 2. The clean surface $1/2$ -order reconstruction in the $[110]$ direction and the $1/4$ -order reconstruction in the $[\bar{1}10]$ direction are shown in Figs. 2(a) and 2(e), respectively. The photographs of these patterns may also be seen in Fig. 1.



FIG. 1. Room-temperature RHEED pattern of (2×4) GaAs (100) in the $[110]$ direction (top), the $[100]$ direction (middle), and $[\bar{1}10]$ direction (bottom).

During the first 0.02–0.20 ML of metal deposition, the RHEED patterns shown in Figs. 2(b) and 2(f) exhibit only the bulk-spaced streaks of the GaAs lattice in the $[110]$ direction with enhanced diffuse scattering (not shown) indicative of disorder in the Al adlayer while a fourfold periodicity persists in the $[\bar{1}10]$ direction. After 0.25 ML Al coverage, the pattern changes to the (4×1) structure [Figs. 2(c) and 2(g)] with no further increase in the diffuse scattering. This reconstruction persists until 0.75 ML coverage, after which traditional Al single-crystal nucleation is observed at coverages less than 4.0 ML. The fully developed Al three-dimensional nucleation at 6.0 ML shown in Figs. 2(d) and 2(h) corresponds to the Al pattern previously reported for deposition onto the (2×4) reconstructed surface.¹¹

A photograph of the RHEED pattern in the $[110]$ direction associated with the (4×1) reconstruction given in Fig. 2(c) is shown in Fig. 3. This fully developed diffraction pattern occurs reproducibly after 0.25 ML of Al deposition. We have found this pattern to exist over the same range of Al coverage at growth rates ranging from 0.017 to 0.050 ML

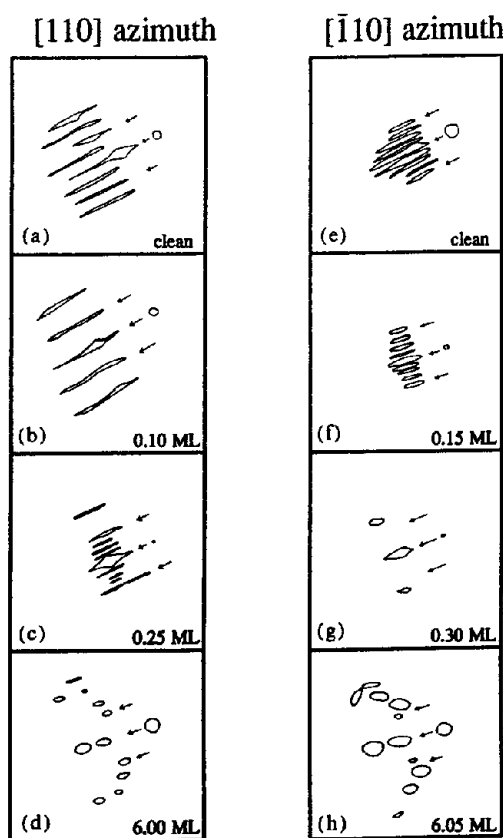


FIG. 2. Schematic representation of the most intense RHEED features vs Al coverage in (a)–(d) the $[110]$ direction and (e)–(h) $[\bar{1}10]$ direction. The clean pattern corresponds to a (2×4) GaAs reconstruction. The (4×1) Al reconstruction is visible in (c) and (g). The fully nucleated Al film is shown in (d) and (h). The arrows indicate the position of the original bulk GaAs streaks. The Al deposition rate was 0.025 ML s^{-1} and the GaAs substrate was held at room temperature.

s^{-1} of Al deposition. A significant amount of disorder on the (2×4) surface, as evidenced by intense curved half-order streaks in the $[100]$ direction, or long-range disorder in the $4 \times$ direction,²⁴ inhibits the formation of the (4×1) reconstruction. Finally, for a well-ordered surface (generally for As-to-Ga ratios of 9:1 to 12:1), the (4×1) reconstruction persists for up to 1 min after the Al oven is shuttered.

The change in interplanar spacing calculated from the position of bulk streaks observed in the RHEED patterns in both the $[110]$ and $[\bar{1}10]$ directions as a function of Al coverage is shown in Fig. 4. In the $[110]$ direction, we find that the interplanar spacing remains at the initial spacing of 4.0 \AA for (2×4) GaAs up to an Al overlayer thickness of $\sim 6 \text{ ML}$. The (2×4) surface has been determined to be roughly 60–70% As^{17–19,25} and the dangling bonds of the As dimers form ideal sites for initial continuation of the bulk crystal. These dimers form perpendicular to the $[110]$ direction and are responsible for the half-order structure observed in this direction on the clean surface. Auger electron spectra indicate that the Al at 0.5 ML coverage exhibits AlAs-like covalently bonded behavior which persists until 3–5 \AA of Al has been deposited.^{8–10} No shift of Ga AES energies toward metallic states was observed for the (2×4) surface²⁶ indicating that no significant Al–Ga bonding exists on this surface. The observation of a $1/4$ -order Al reconstruction in this direction combined with the Auger observations implies an association of Al with these dimers. At a film thickness of ~ 6



FIG. 3. RHEED pattern with 1/4-order periodicity in the [110] direction after 0.25 ML of Al deposition.

ML, additional spots appear corresponding to a lattice spacing of 2.86 Å, representing the mixed nucleation of Al(110) + Al(001) as seen in Figs. 2(d) and 2(h) and in agreement with previous studies.^{11,12} Very different results are found along the $\bar{1}10$ direction. As shown in Fig. 4, there is an increase in the spacings between the bulk streaks which implies that the interplanar spacing decreases from 4.0 to 2.91 Å at a coverage of 0.17 ML of Al. This striking result shows that there is a strong, directionally dependent metal-metal interaction with Al only weakly interacting with the surface. The bulk Al spacing of 2.86 Å (nearest-neighbor distance in the fcc metal) is achieved after a coverage of only 0.30 ML. The strong adatom-adatom interaction accompanied by the (4×1) reconstruction implies that the first Al atoms in this direction probably occupy the channels between pairs of dimers. For a highly disordered surface, this strong adatom-adatom interaction does not occur. In this case, the interplanar spacings in both directions remain fixed at 4.0 Å characteristic of predominant Al(100) growth. The Al structure in the $\bar{1}10$ direction after 0.30 ML in Fig. 2(g) may be similar to the very low coverage nucleation of Ag observed in the $\bar{1}10$ direction during Ag deposition onto (2×4) GaAs(001).²⁷

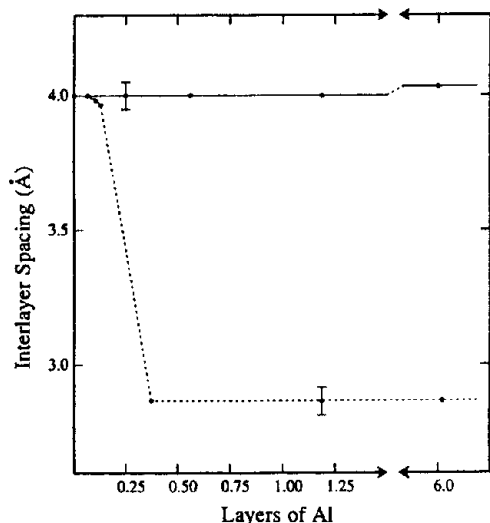


FIG. 4. Bulk interplanar spacing as a function of Al coverage in the [110] (solid line) and $\bar{1}10$ (dashed line) directions, as determined in part from the data shown in Fig. 2. The Al deposition rate was 0.025 ML s^{-1} and the GaAs substrate was held at room temperature.

In conclusion, we have shown that Al can form a highly ordered overlayer with (4×1) symmetry in the low coverage regime crucial to Schottky barrier formation for metals on GaAs. This geometrical configuration may give an indication of the stability of these surfaces with respect to very small numbers of adatoms. The directional dependences indicated by the (4×1) reconstruction, which result in quarter-order periodicity of chemisorbed atoms and bulk-like periodicity of Al atoms for which the metal-metal interaction is stronger, may help quantify the extent of charge transfer at the Al/GaAs(001) interface during the barrier formation process. It will be interesting to further pinpoint the Al locations using more precise surface structure techniques such as scanning tunneling microscopy or ion scattering.

The authors gratefully acknowledge the financial support of the Office of Naval Research, the National Science Foundation, and the IBM Corporation. We also thank Andrea Schmalz for help in obtaining Fig. 2.

¹For a comprehensive review of the subject of metal-semiconductor interfaces, see L. J. Brillson, *Surf. Sci. Rep.* **2**, 123 (1982).

²A. Zunger, *Phys. Rev. B* **24**, 4372 (1981), and references therein.

³W. E. Spicer, P. W. Chye, P. R. Skeath, C. Y. Su, and I. Lindau, *J. Vac. Sci. Technol.* **16**, 1422 (1979); **17**, 1019 (1980); *Phys. Rev. Lett.* **44**, 420 (1980); *J. Vac. Sci. Technol. B* **6**, 1245 (1988).

⁴O. F. Sankey, R. E. Allen, S.-F. Ren, and J. D. Dow, *J. Vac. Sci. Technol. B* **3**, 1162 (1985).

⁵R. E. Viturro, J. L. Shaw, C. Mailhot, L. J. Brillson, N. Tache, J. McKinley, G. Margaritondo, J. M. Woodall, P. D. Kirchner, G. D. Pettit, and S. L. Wright, *Appl. Phys. Lett.* **52**, 2052 (1988), and references therein.

⁶S. V. Svensson, J. Kanski, T. G. Andersson, and P. O. Nilsson, *Surf. Sci.* **124**, L31 (1983); *J. Vac. Sci. Technol. B* **2**, 235 (1984).

⁷L. J. Brillson, R. E. Viturro, C. Mailhot, J. L. Shaw, N. Tache, J. McKinley, G. Margaritondo, J. M. Woodall, P. D. Kirchner, G. D. Pettit, and S. L. Wright, *J. Vac. Sci. Technol. B* **6**, 1263 (1988).

⁸R. Ludeke and G. Landgren, *J. Vac. Sci. Technol.* **19**, 667 (1981).

⁹G. Landgren and R. Ludeke, *Solid State Commun.* **37**, 127 (1981).

¹⁰G. Landgren, S. P. Svensson, and T. G. Andersson, *Surf. Sci.* **122**, 55 (1982).

¹¹G. Landgren, R. Ludeke, and C. Serrano, *J. Cryst. Growth* **60**, 393 (1982).

¹²R. Ludeke, L. L. Chang, and L. Esaki, *Appl. Phys. Lett.* **23**, 201 (1973).

¹³J. Massies, J. Chaplart, and N. T. Linh, *Solid State Commun.* **32**, 707 (1979).

¹⁴J. Massies and N. T. Linh, *Surf. Sci.* **114**, 147 (1982).

¹⁵L. J. Brillson, C. F. Brucker, A. D. Katnani, N. G. Stoffel, and G. Margaritondo, *J. Vac. Sci. Technol.* **19**, 661 (1981).

¹⁶R. Blumenthal, S. K. Donner, J. L. Herman, R. Trehan, K. P. Caffey, E. Furman, B. D. Weaver, and N. Winograd, *J. Vac. Sci. Technol. B* **6**, 1444 (1988).

¹⁷J. Massies, P. Etienne, F. Dezaly, and N. T. Linh, *Surf. Sci.* **99**, 121 (1980).

¹⁸R. Z. Bachrach, R. S. Bauer, P. Chiaradia, and G. V. Hansson, *J. Vac. Sci. Technol.* **19**, 335 (1981).

¹⁹F. Briones, D. Golmayo, L. Gonzalez, and J. L. DeMiguel, *Jpn. J. Appl. Phys.* **24**, L478 (1985).

²⁰J. J. Harris, B. A. Joyce, and P. J. Dobson, *Surf. Sci.* **103**, L90 (1981).

²¹Riber MBE Instruction Manual, April, 1985.

²²J. H. Neave and B. A. Joyce, *J. Cryst. Growth* **44**, 387 (1978).

²³B. A. Joyce, J. H. Neave, P. J. Dobson, and P. K. Larsen, *Phys. Rev. B* **29**, 814 (1984).

²⁴S. K. Donner, K. P. Caffey, and N. Winograd, *J. Vac. Sci. Technol. B* **7**, 742 (1989).

²⁵P. Drathen, W. Ranke, and K. Jacobi, *Surf. Sci.* **77**, L162 (1978); R. Z. Bachrach, R. S. Bauer, P. Chiaradia, and G. V. Hansson, *J. Vac. Sci. Technol.* **18**, 797 (1981); R. Ludeke, T.-C. Chiang, and D. E. Eastman, *Physica B* **117&118**, 819 (1983).

²⁶T. G. Andersson, S. P. Svensson, and G. Landgren, *J. Vac. Sci. Technol. B* **1**, 361 (1983).

²⁷R. Ludeke, *Surf. Sci.* **132**, 143 (1983).